Society For Biomaterials

TiO_2-coated CoCrMo: Improving the osteogenic differentiation and adhesion of mesenchymal stem cells *in vitro*

Niall Logan,[1] Anas Sherif,[1] Alison J. Cross,[2] Simon N. Collins,[3] Alison Traynor,[3] Laurent Bozec,[1] Ivan P. Parkin,[2] Peter Brett[1]

[1]Biomaterials and Tissue Engineering, University College London, Eastman Dental Institute, London WC1X 8LD, United Kingdom
[2]Department of Chemistry, University College London, London WC1H 0AJ, United Kingdom
[3]Corin Ltd, Cirencester, Gloucestershire GL7 1YJ, United Kingdom

Received 15 May 2014; revised 2 June 2014; accepted 10 June 2014
Published online 19 August 2014 in Wiley Online Library (wileyonlinelibrary.com). DOI: 10.1002/jbm.a.35264

Abstract: The current gold standard material for orthopedic applications is titanium (Ti), however, other materials such as cobalt–chromium–molybdenum (CoCrMo) are often preferred due to their wear resistance and mechanical strength. This study investigates if the bioactivity of CoCrMo can be enhanced by coating the surface with titanium oxide (TiO_2) by atmospheric pressure chemical vapor deposition (CVD), thereby replicating the surface oxide layer found on Ti. CoCrMo, TiO_2-coated CoCrMo (CCMT) and Ti substrates were used for this study. Cellular f-actin distribution was shown to be noticeably different between cells on CCMT and CoCrMo after 24 h in osteogenic culture, with cells on CCMT exhibiting greater spread with developed protrusions. Osteogenic differentiation was shown to be enhanced on CCMT compared to CoCrMo, with increased calcium ion content per cell ($p < 0.05$), greater hydroxyapatite nodule formation ($p < 0.05$) and reduced type I collagen deposition per cell ($p < 0.05$). The expression of the focal adhesion protein vinculin was shown to be marginally greater on CCMT compared to CoCrMo, whereas AFM results indicated that CCMT required more force to remove a single cell from the substrate surface compared to CoCrMo ($p < 0.0001$). These data suggest that CVD TiO_2 coatings may have the potential to increase the biocompatibility of CoCrMo implantable devices. © 2014 Wiley Periodicals, Inc. J Biomed Mater Res Part A: 103A: 1208–1217, 2015.

Key Words: osteogenesis, titanium oxide, cobalt alloy, AFM, mesenchymal stem cells

How to cite this article: Logan N, Sherif A, Cross AJ, Collins SN, Traynor A, Bozec L, Parkin IP, Brett P. 2015. TiO_2-coated CoCrMo: Improving the osteogenic differentiation and adhesion of mesenchymal stem cells *in vitro*. J Biomed Mater Res Part A 2015:103A:1208–1217.

INTRODUCTION

The medical health care industry is constantly improving, providing more accurate methods of diagnosis and more effective therapeutic treatments. A consequence of this is that people are living for longer, creating an ever growing elderly population, which is affecting all fields of health care, both clinically and economically.[1] Included in this trend is orthopedics, which is predicted to see a 174 and 673% rise in the need for total hip and knee arthroplasty procedures by the year 2030, respectively.[2–4] As a result of this, the need for improvements in current generation biomaterials is of great interest and importance to both the scientific and medical industries, as implants that are capable of increased longevity and biocompatibility are desired. At present, titanium (Ti) and its alloys are widely accepted as the prime choice for orthopedic and dental applications.[5,6] This is due to a combination of desirable properties that include, resistance to corrosion, mechanical strength and biocompatibility that is capable of promoting an environment that can trigger the formation of new bone tissue and osseointegration.[7,8] While these characteristics make Ti the material of choice, it is not always suitable for some applications. Other biomaterials, such as the cobalt alloy, cobalt–chromium–molybdenum (CoCrMo), can often be preferred due to their superior mechanical strength and wear resistance; however they do not exhibit the same osteogenic ability as Ti. Efforts to improve the efficacy of CoCrMo have included acid etching,[9] diamond like carbon films,[10] bone-morphogenetic protein peptide immobilization,[11] and nanophase topography[12]; however, these methods are either largely ineffective or difficult to upscale effectively.

On implantation, the bone surrounding the implant does not 'see' the bulk of the metal, but instead interacts with the stable oxide layer found on the surface of Ti and its alloys. At approximately 3–7 nm thick,[13] this thin, durable, self-repairing oxide layer could play an important role in the osseointegration of the implant by mediating cell–surface interactions such as, protein adsorption, cell adhesion and differentiation, and eventually bone formation and remodeling. This has led us to develop a novel approach to

Correspondence to: P. Brett; e-mail: p.brett@ucl.ac.uk
Contract grant sponsors: EPSRC, Molecular Modelling and Materials Science Engineering Doctorate Centre UCL, and Corin Ltd (Cirencester, UK)

increasing the biocompatibility of CoCrMo by coating the material in a highly durable layer of TiO_2 by atmospheric pressure chemical vapor deposition (CVD) in order to replicate the surface of Ti implants and so enhance the osseointegration of these CoCrMo components. Current applications of this coating include use as a heterogeneous catalyst, a photo-catalyst in solar cells, white pigment in paint, gas sensors, anticorrosion protective coatings, optical coatings, and varistors for electrical devices.[14]

To investigate the osteogenic capability of TiO_2 coatings, the biological activity of human mesenchymal stem cells (MSCs) isolated from the bone marrow of the iliac crest were studied. MSCs, also referred to as, mesenchymal stromal cells and skeletal stem cells, are multipotent cells capable of self-renewal, with the potential to differentiate into a variety of specialized cell types, such as osteoblasts, chondrocytes, and adipocytes.[15] Following implantation, MSCs are the first osteogenic cells recruited to such sites *in vivo*, where they facilitate in the formation of a direct interface between native bone tissue and the implant by colonizing the surrounding tissues and surfaces and differentiating into osteoblasts capable of forming new bone tissue.[16,17]

The present study sought to observe the effects of CoCrMo, TiO_2-coated CoCrMo (CCMT), and Ti surfaces on the osteogenic differentiation of human MSCs by analyzing specific markers known to play a role in osteogenesis, including cytoskeletal structure, calcium deposition, type I collagen (COL-I), and hydroxyapatite (HA) formation. In addition to studying factors involved in differentiation, cell attachment and adhesion was examined to further assess the properties of the surfaces, as adhesion is known to play a pivotal role in the differentiation process.[18] A novel approach involving AFM following a 1-s dwell time on each substrate was used to measure single cell adhesion forces.[19] We hypothesise that the CCMT surface will display similar behavior to that of the Ti surface, in the form of enhancing cell adhesion and promoting greater expression of osteogenic markers.

MATERIALS AND METHODS

Sample preparation

CoCrMo discs (Cr 26–30, Mo 5–7) of 15 mm Ø, 1 mm thickness, were supplied by Corin (Cirencester, UK) with a machined finish. To remove this topography, individual discs were mounted on resin bases (SpeciFix-20, Struers, 40200048) and fixed in place using araldite rapid for 30 min. Once the discs were securely fixed, using a LaboForce-1 grinding machine (Struers) the surface of the discs were manually ground with SiC #1000 grit paper (Struers, 40400011) to remove any visible appearance of the machined topography. Following this, discs were transferred to a RotoForce-1 polishing machine (Struers) and polished for 4.5 min at 150 rpm using MD-Dac (Struers, 40500071) with DP-Suspension P 3μm (Struers, 40600251) while lubricating the samples with DP-Lubricant Blue (Struers, 40700006). The CoCrMo discs were then immersed in an ultrasound bath containing $_{dd}H_2O$ for 30 min and air dried. Ti discs were provided by Institut Straumann AG (Waldenberg, Switzerland). To prepare CoCrMo, CCMT, and Ti discs for cell culture experiments, discs were put in nitric acid (0.1 N, BDH, 19088 5E) for 10 min, washed thoroughly in $_{dd}H_2O$ and allowed to air dry before being UV irradiated for 20 min on each side (BONMAY, BR-506).

Chemical vapor deposition

Titanium tetrachloride ($TiCl_4$) and ethyl acetate were used to create the thin film TiO_2 coatings on CoCrMo via atmospheric pressure CVD. The process followed a procedure developed by us previously to coat both glass and steel substrates.[20,21] The $TiCl_4$ bubbler was heated to 68°C and ethyl acetate heated to 40°C. All gas lines were heated to over 150°C and the deposition was carried out at a temperature of 500°C. In each deposition approximately 30 CoCrMo discs were placed on an inert glass tray, and arranged to be close to the gas inlet of the reaction chamber. The flow rates for the 1 min deposition were 1.32 L/min for $TiCl_4$, 0.3 L/min for ethyl acetate, 3 L/min for plain 1, and 1.85 L/min for plain 2. X-ray diffraction, X-ray photoelectron spectroscopy, and Raman spectroscopy was performed to confirm the presence of anatase TiO_2 (not shown here).

Surface characterization

The surface topography of CoCrMo, CCMT, and Ti were analyzed by profilometry (Scantron, Proscan 1000) where an area of 6.25 mm^2 was examined ($n = 5$) and using Proscan software, surface roughness was evaluated to obtain R_a values. Scanning electron microscopy was used to visually confirm surface R_a values. To measure the hydrophobicity of the samples ($n = 6$), contact angle measurements were performed using an optical contact angle meter (KSV Instruments, CAM 200) with drops of $_{dd}H_2O$.

Cell culture

Human MSCs from three donors were obtained from the Institute for Regenerative Medicine, Texas A&M Health Science Center College of Medicine. Precharacterization of the MSCs had been performed which included the expression of stem cell surface markers, and osteogenic, adipogenic, and chondrogenic differentiation. Cells were seeded on tissue culture plastic at a density of 740 cells cm^{-2} and expanded in complete growth medium (CGM) that comprised of minimum essential medium α (Gibco, 22571-020) containing 10% fetal bovine serum (PAA Laboratories, A15-151) and 1% penicillin/streptomycin (PAA Laboratories, P11-010). MSCs were incubated at standard culture conditions of 37°C/5%CO_2 in a humidified atmosphere with media changed every 3 or 4 days. When cells reached 80% confluence they were harvested by treatment of trypsin (0.05%)/ethylenediaminetetraacetic acid (0.002%; PAA Laboratories, L11-004). Only cells of low passage (<5) were used to ensure integrity of the results. When osteogenic media (OM) was implemented, it consisted of Dulbecco's modified Eagle's medium (DMEM) low glucose pyruvate (Gibco, 31885-023), containing 10% fetal bovine serum, 1% penicillin/streptomycin, and further supplemented with β-glycerol phosphate (Sigma-Aldrich,

G9891), L-ascorbic acid (Sigma-Aldrich, A8960), and dexamethasone (Sigma-Aldrich, D9402).

Cell morphology

To analyze cell morphology, f-actin and the nuclei of MSCs were fluorescently labeled to undergo confocal laser microscopy. MSCs were seeded on CoCrMo and CCMT discs at 12.5 $\times$ 10^3 cells per well in OM ($n = 3$) with media changes every 3–4 days. After 1 and 7 days in culture, MSCs were fixed using 4% paraformaldehyde for 15 min then treated with 0.15% Triton X-100 (BDH, 30632 4N) in Dulbecco's phosphate buffer saline (PBS; Lonza, 17-512F) for 4 min to permeabilize the cellular membrane. Actin was labeled using Alexa fluor 488 phalloidin in PBS (Molecular probes, A12379, 2.5:100) for 20 min at room temperature, then counterstained to label the nuclei using propidium iodide (PI) for 10 min (Molecular probes, P3566, 4 μg/mL). Cells were washed three times in PBS and suspended in 3 mL of PBS in for viewing. MSCs were analyzed at ×40, using a Radiance 2100 Laser Scanning System.

Osteogenic fluorescent markers

To obtain a measure of the level of osteogenic differentiation occurring in MSCs on the three surfaces, COL-I and HA expression were examined using fluorescent microscopy techniques. MSCs were seeded at 12.5 $\times$ 10^3 cells per well in OM ($n = 3$) with media changes every 3–4 days. COL-I was analyzed after 7 and 14 days, with HA being studied after 7, 14, and 21 days. Succeeding culture, cells were fixed as previously described. MSCs to be analyzed for COL-I were blocked using 10% goat serum (Sigma-Aldrich, G9023) in PBS for 30 min to prevent any unspecific binding. Primary antibody incubation was performed overnight at 4°C with anti-COL-I antibody (Sigma-Aldrich, C2456, 1:1000). Alexa fluor 488 goat anti-mouse (Molecular probes, A11001, 2.5:100) was used as a secondary antibody to label COL-I, with all primary and secondary antibodies diluted in 1.5% skim milk in PBS. Lastly, the MSCs were counterstained with 4′,6-diamidino-2-phenylindole dihydrochloride (DAPI) for 40 min (Sigma-Aldrich, D9542, 10 μg/mL). HA staining was performed using the OsteoImage kit (Lonza, PA-1503) as per the manufacturer's instructions. Images were taken using a fluorescent microscope fitted with the appropriate filters (Leica DMIRB) and then quantifiable analysis was performed via a pixel based method using ImageJ software.

Calcium ion content

MSCs from three donors were seeded at a density of 12.5 $\times$ 10^3 cells per well in OM and examined at 7, 14, and 21 days. Prior to performing assays, the amounts of cells were assessed using AlamarBlue (AbD Serotec); oxidized dye was added to each well containing media and cells were incubated for 4 h at standard culture conditions before having two aliquots of supernatant removed from each well for analysis. The fluorescent intensity of the dye was measured (excitation $\lambda = 530$ nm, emission $\lambda = 590$ nm, Biotek FLX800) and cell numbers calculated via interpolation through use of a seven-point standard curve, ranging up to a maximum of 16 $\times$ 10^4 cells per well. Calcium content was measured using the QuantiChrom assay (Bio Assay systems, DICA-500) as per the manufacturer's instructions. The cell monolayer was homogenized by incubation with 1 *M* hydrochloric acid (HCL) for 60 min at room temperature on a rocking plate. Aliquots were then taken from each sample and transferred to a clear 96-well plate and combined with assay reagent. Calcium levels were then measured ($\lambda = 620$ nm, Tecan M200) and concentrations calculated with use of known concentration standards.

Vinculin expression

The focal adhesion (FA) protein vinculin was analyzed using confocal laser microscopy to obtain a level of expression on the three surfaces after 3 and 24 h in osteogenic culture. MSCs were seeded at 5 $\times$ 10^3 cells per well ($n = 3$) and succeeding culture were prepared as previously described, although they were immunochemically stained with the mouse antivinculin antibody (Abcam, ab18058, 1:200) and Alexa fluor 568 goat anti-mouse secondary antibody (Molecular probes, A11031, 2.5:100). MSCs were then washed and viewed in 3 mL of PBS at ×40, using a Radiance 2100 Laser Scanning System. Vinculin expression in individual cells was then quantified as a pixel based method using ImageJ software.

Atomic force microscopy

A total of 1 $\times$ 10^3 MSCs were transferred to a 35-mm Petri dish containing one disc of CoCrMo, CCMT, and Ti in CGM. The Petri dish was then inserted into the heater chamber on the NanoWizard AFM stage (JPK—Berlin) to maintain the cells at 37°C, and the medium was replaced with long lasting CO_2 serum free medium (Sigma Aldrich, 14571C). In order to perform the experiment, we modified AFM nonconductive silicon nitride tip-less cantilevers (Bruker, NP-010) with glass beads (10–30 μm, Polysciences, 07666) which had been coated with concanavalin A (Con A) biomolecules as previously described.[19] The AFM cantilever was then approached to a single free moving MSC with a maximum load varying between 400 and 900 pN to ensure contact adhesion between the cell and the modified bead. This load was also low enough to prevent any compressive damage to the cell. The cantilever was then retracted and left undisturbed for 15 min to ensure strong adhesion between the cell and the coated glass bead. Following these preparation steps, adhesion measurements were performed between the modified cantilever/bead/cell and different surfaces of interest by performing force–distance curves using the AFM. The single cell adhesion measurements were performed using an initial load of 4.5 nN, a dwell time of 1 s and a retraction loading rate of 0.5 μm/s. At all times the sample and cell were kept in a buffered environment (DMEM) at 37°C and 5% CO_2. Attachment of the MSC to the Con A coated glass bead was confirmed by SEM and the AFM camera.

Statistical analysis

For each experiment samples were performed in triplicate ($n = 3$) except for surface characterization analysis which used a sample size of $n = 6$ for contact angle and $n = 5$ for

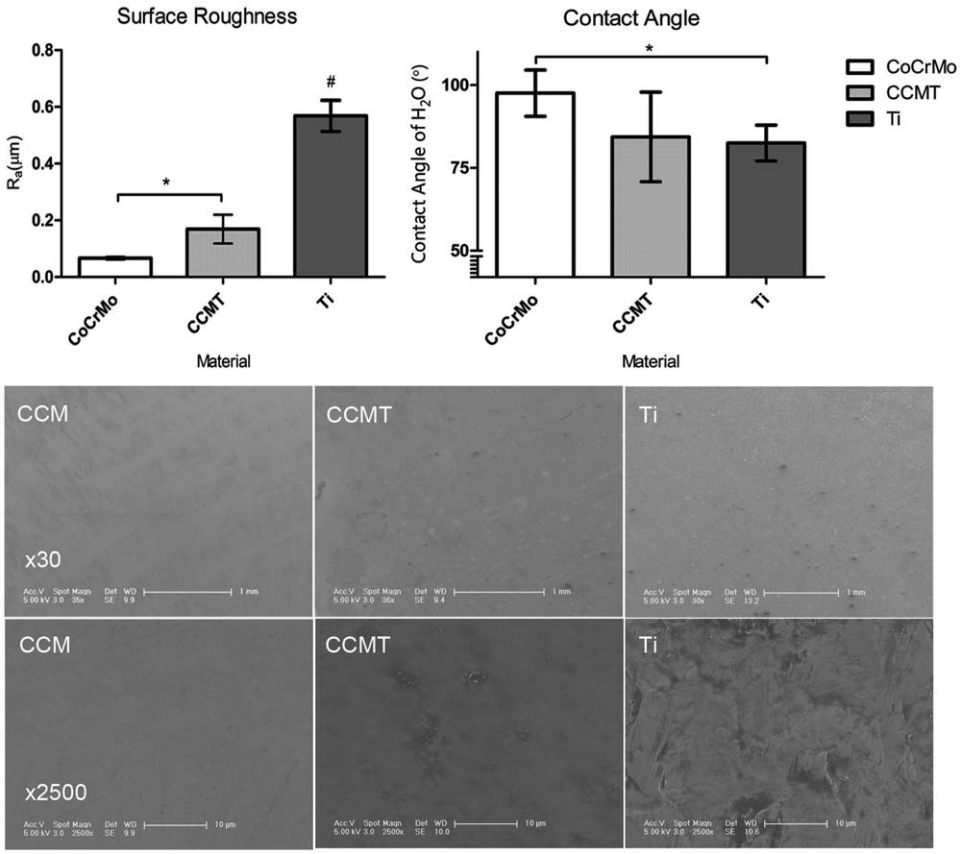

FIGURE 1. Above left—surface roughness results, showing significantly greater roughness on the Ti surface against both CoCrMo and CCMT, and also a significant increase in roughness on the CCMT surface in comparison to the CoCrMo ($n = 5$). Above right—Contact angle results, CoCrMo surface is significantly more hydrophobic than Ti, with the CCMT surface ranging in the middle of the two ($n = 6$). Below—SEM images taken on all three surface variants at magnification ×30 and ×2500. At lower magnification (×30) all three surfaces appear similar in appearance which could be described as smooth. Under greater magnification (×2500) differences between the surfaces is more apparent, increasing in roughness from CoCrMo–CCMT–Ti respectively, supporting the laser profiliometer results. Each bar represents the mean ± 1SD, *$p < 0.05$ material versus one surface, #$p < 0.05$ material versus both surfaces.

roughness. Quantification of vinculin expression was performed using 10 cells ($n = 10$). Using GraphPad Prism software the Student's t test was used to examine the statistical significance between groups with $p < 0.05$ to be considered significant.

RESULTS

Surface characterization

As shown in Figure 1, CoCrMo was the most hydrophobic of the three surfaces with a mean contact angle of $97.5 \pm 7°$. Ti had the lowest contact angle, with a mean of $82.5 \pm 5.4°$ and CCMT averaged in the middle of the group with a mean of $84.3 \pm 13.5°$. CoCrMo was observed to have a significantly greater contact angle than Ti. Ti was shown to have significantly greater surface roughness (R_a 0.56 ± 0.055 μm) than both CoCrMo (R_a 0.07 ± 0.004 μm) and CCMT (R_a 0.17 ± 0.050 μm), whereas CCMT also had a significant upregulation in comparison against CoCrMo. Although there was significant differences in R_a values between the three surfaces, all three surfaces can be referred to as smooth when taken into consideration past publications and the given roughness ranges referred to as smooth in a review by Wennerberg et al.[22] SEM analysis of surface topography, shown in Figure 1, supported the laser profilometry results, where at low magnification (X30), each surface appeared smooth, lacking any topography, but at greater magnification (X2500), the increased roughness was evident on the CCMT and Ti surfaces.

Cell Morphology

Laser confocal microscopy was used to analyze the cell morphology of MSCs seeded on CoCrMo and CCMT. After 24 h culture in OM, there were obvious differences in the appearance of MSC f-actin which had been fluorescently labeled with phalloidin. Where cell aggregates had formed, the structure and order of cells within these colonies were evidently different between the surfaces. Aggregates on CoCrMo [Fig. 2–(A)] appeared to have thin stress fibres, which were elongated and ordered in parallel to each other, whereas on CCMT [Fig. 2(D)], stress fibres seemed to be more robust and were disorganized in a crisscross manner. The morphological differences observed in cell aggregates on CoCrMo and CCMT after 24 h was also evident in individual cells. The majority of MSCs on the CoCrMo surface appeared fibroblastic in appearance

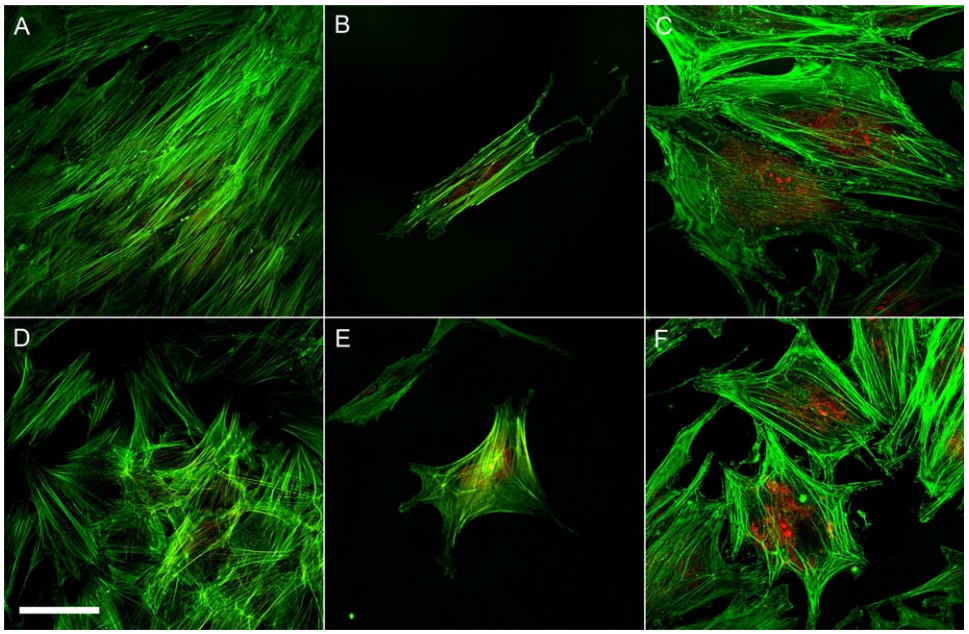

FIGURE 2. Confocal images showing f-actin (green) counterstained with PI (red). Images (A)–(C) show MSCs cultured in OM on CoCrMo, with cell aggregates at day 1 (A), single cells at day 1 (B), and single cells at day 7 (C). Images (D)-(F) show MSCs on the CCMT surface, with aggregates at day 1 (D), single cells at day 1 (E), and single cells at day 7 (F). Cell morphology at day 1 is noticeably different in both aggregates and on the single cell level. Aggregates on CoCrMo appear to have ordered, elongated, parallel stress fibres, in comparison to the more robust criss-cross fibres found on the CCMT surface. Scale bar = 50 μm. [Color figure can be viewed in the online issue, which is available at wileyonlinelibrary.com.]

[Fig. 2(B)], in comparison to MSCs found on the CCMT surface which appeared more spread, with developed protrusions in the form of lamellipodia [Fig. 2–(E)]. After 7 days in osteogenic culture, the morphology of MSCs on CoCrMo and CCMT [Fig. 2(C,F)] had significantly changed from day 1 as MSCs had undergone the differentiation process. MSCs on both surfaces were noticeably more well spread, with the formation of thick bundles of actin around the periphery of the cells, a trait seen before in MSCs undergoing osteogenesis.[23] While MSCs were evidently different from images taken at day 1, no obvious difference in cell morphology was present between surfaces at day 7.

Osteogenic fluorescent markers

As MSCs differentiate into osteoblastic cells capable of forming new mineralized bone tissue, they undergo a complex series of events which includes the alteration of their physical form, production and expression of osteogenic proteins capable of facilitating in osteogenesis, and the excretion of a collagenous extracellular matrix (ECM) rich in calcium nucleation sites. Fluorescent microscopy techniques were used to monitor a selection of these events to gain an understanding of each surface's ability to promote osteogenesis *in vitro*. COL-I is thought to be excreted into the ECM of MSCs that are undergoing osteogenic differentiation to act as a scaffold for tissue formation. After 7 days in osteogenic culture, it was apparent that COL-I deposition was significantly enhanced on the CoCrMo surface, shown by the presence of dense collagen fibrils [Fig. 3(A)], which were not present to the same extent on either CCMT or Ti [Fig. 3(B,C)]. After 14 days in culture this effect was again observed on CoCrMo, although at this time point, CCMT was shown to have significantly more COL-I per cell deposited compared to Ti, while not to the same level as CoCrMo [Fig. 3(D)]. HA, also called hydroxylapatite (HA; $Ca_5((PO_4)(OH))$, is a mineral naturally found in bone tissue and can be used as a late marker for osteogenesis, as MSCs produce nodules of HA as they form new bone tissue. Ti promoted the greatest amount of HA formation throughout the 3-week time course, being statistically significant over both materials at 2 weeks and CoCrMo at 3 weeks. Noticeably larger nodules were evident on Ti [Fig. 4(C)], while CCMT was shown to have greater HA content over CoCrMo at all three time points but at 3 weeks this was deemed statistically significant [Fig. 4(D)].

Calcium deposition

To combine with the fluorescent microscopy techniques that analyzed known markers of osteogenic differentiation, calcium ion content was quantitatively determined through use of a colorimetric assay. Use of Alamarblue prior to assaying allowed for results to be normalized to a per cell level instead of total content, to allow for greater accuracy. As shown in Figure 5, after 2 weeks in osteogenic culture CCMT and Ti had significantly greater calcium ion content per cell in comparison against CoCrMo, implying MSCs on these substrates are differentiating at a faster rate and producing more mineralized tissue. This trend was again evident at 3 weeks, although not deemed to be statistically significant for CCMT.

Vinculin

Using confocal laser microscopy, vinculin expression in MSCs was analyzed after 3 and 24 h in osteogenic culture and then

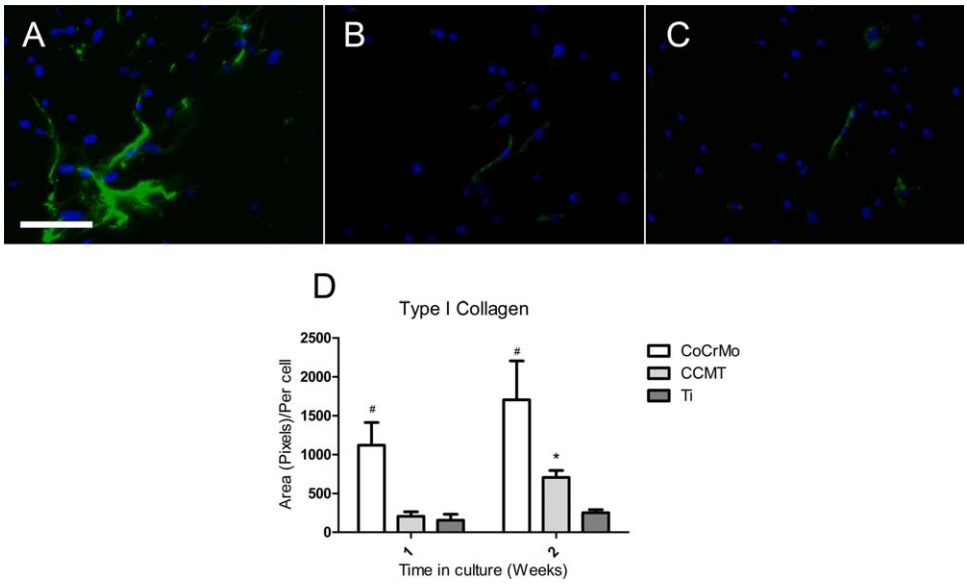

FIGURE 3. Fluorescent images and quantification analysis for COL-I (A–D) after 7 days in culture. COL-I deposition was enhanced on the CoCrMo surface (A), shown by the formation of dense collagen fibrils (green), which were not present on either CCMT (B) or Ti (C). Cultures were counterstained with the nucleic acid stain DAPI (blue). Scale bar = 100 μm. Image quantification analysis was performed using ImageJ software (D) $n = 8$. Each bar represents the mean ± 1SD, $*p < 0.05$ material versus one surface, and $\#p < 0.05$ material versus both surfaces. [Color figure can be viewed in the online issue, which is available at wileyonlinelibrary.com.]

quantified as a pixel based method using individual cells of comparable size [Fig. 6(D)]. Ti appeared to promote the greatest expression of vinculin at both time points, and was judged to be statistically significant against CoCrMo at 24 h. CCMT appeared to have greater vinculin expression than CoCrMo at both 3 and 24 h, although to a lesser extent than that found on Ti. Congregation of vinculin at FAs was present on all three surfaces [Fig. 6(A–C)], although Ti and CCMT appeared to have a greater number FAs per cell, which indicates that MSCs on these surfaces may be more well adhered.

Atomic force microscopy

AFM was used to analyze the force required to detach a single MSC from the surface of CoCrMo, CCMT, and Ti following a 1-s dwell time. In doing this experiment it was possible to gain an understanding of each substrates ability to promote immediate cellular adhesion, which is a necessity for osteogenesis to occur successfully on implants *in vivo,* as colonization of cells with osteogenic potential is required on the surface of an implant. It was found that there were statistically significant differences between all three surfaces

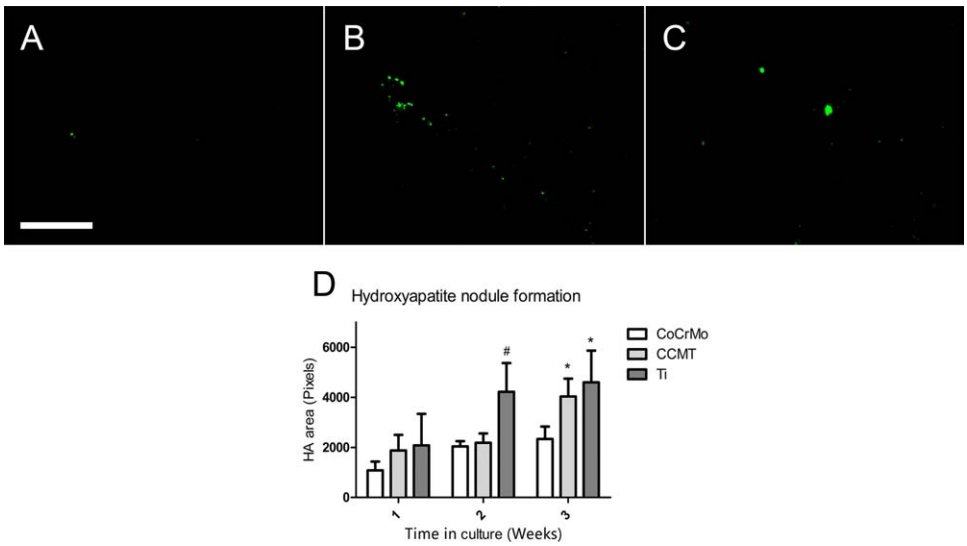

FIGURE 4. HA nodule formation was shown to be greater on CCMT (B) and Ti (C) in comparison to CoCrMo (A) after 21 days in culture. Quantification analysis was performed using ImageJ software (D) $n = 10$. HA shown as green (A–C), scale bar = 200μm. Each bar represents the mean ± 1SD, $*p < 0.05$ material versus one surface, and $\#p < 0.05$ material versus both surfaces. [Color figure can be viewed in the online issue, which is available at wileyonlinelibrary.com.]

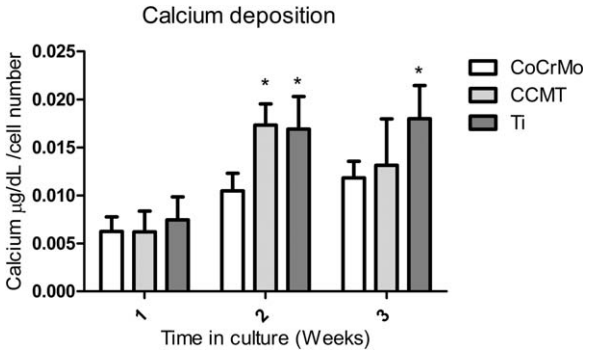

FIGURE 5. Calcium deposition per cell over a 3-week time course. At 2 weeks, there is a significant increase in the amount of calcium present on CCMT in comparison to CoCrMo, suggesting a greater level of osteogenesis is occurring at this time point on the CCMT surface, to a similar level as that found on Ti. At 3 weeks, there is still greater calcium content on CCMT although not statistically significant. Each bar represents the mean ± 1SD $n = 3$, $*p < 0.05$ material versus CoCrMo.

(Fig. 8, $p < 0.0001$), with CoCrMo requiring the lowest detachment force (29.22 ± 1.36 nN), CCMT ranging in the middle (31.58 ± 1.60 nN), and Ti requiring the greatest force (32.65 ± 1.57 nN). This implies that Ti promotes greater immediate adhesion to a statistically superior level than both other surfaces, which can also be said for CCMT against CoCrMo.

DISCUSSION

The demographics of the United Kingdom show the population is changing rapidly with mean age increasing as people

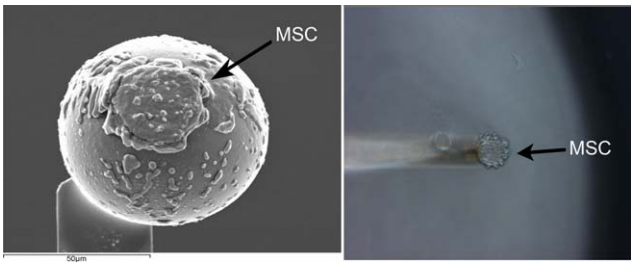

FIGURE 7. SEM and AFM camera images showing a single MSC attaching to a Con A-coated glass beaded AFM cantilever. [Color figure can be viewed in the online issue, which is available at wileyonlinelibrary.com.]

are living for longer.[1] Consequently, implant lifespans that were once considered acceptable are no longer so, as patients are out-living their devices. Upon failure of the implant, the need for invasive revision surgery is common, which can cause significant additional trauma to the patient, as well as add substantial cost to health care provider.[3,4] Implantable devices that exhibit increased longevity and biocompatibility are therefore being sought in order to meet the needs of this growing, aging population. Many research groups are currently looking into various methods of modifying current generation biomaterials to enhance their performance *in vivo*. One such material in question is the cobalt alloy, CoCrMo, which is currently used in orthopedic applications due to its mechanical strength and excellent resistance to wear. While CoCrMo exhibits these excellent properties, it does not have the *in vivo* biological compatibility of materials such as Ti. In the present study we investigated if the biocompatibility of CoCrMo could be improved

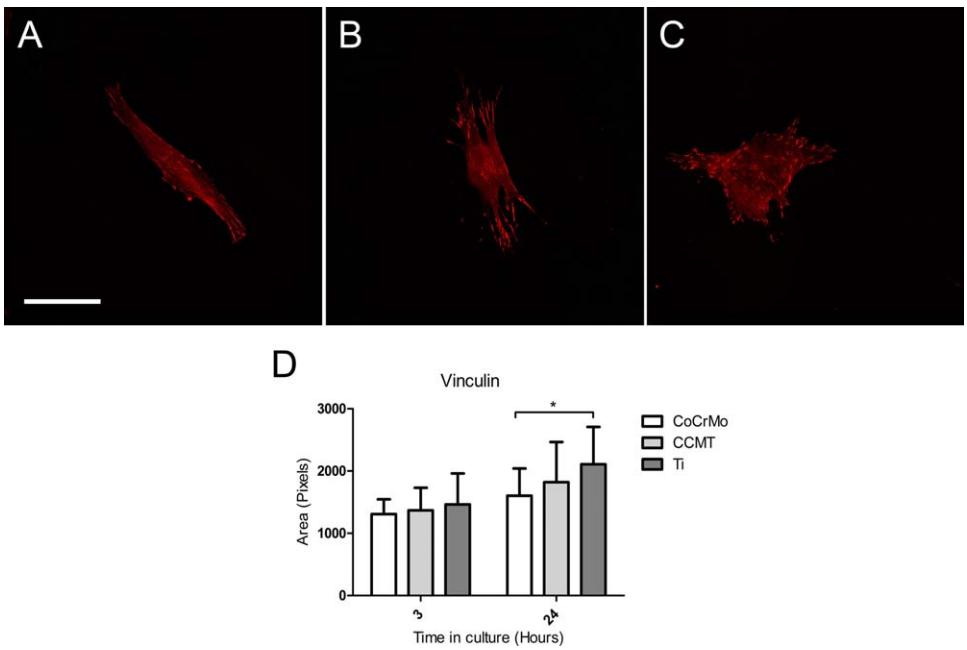

FIGURE 6. Vinculin expression in MSCs on CoCrMo (A), CCMT (B), and Ti (C) after 24 h in culture. Fluorescent images show vinculin expression throughout the cell with concentrated regions thought to represent focal adhesions. Quantification of vinculin expression in individual cells (D) was performed using ImageJ software where it was found Ti had greater vinculin present in comparison to CoCrMo, with CCMT ranging in the middle. Each bar represents the mean ± 1SD $n = 10$, $*p < 0.05$ material versus CoCrMo. Scale bar = 50 µm. [Color figure can be viewed in the online issue, which is available at wileyonlinelibrary.com.]

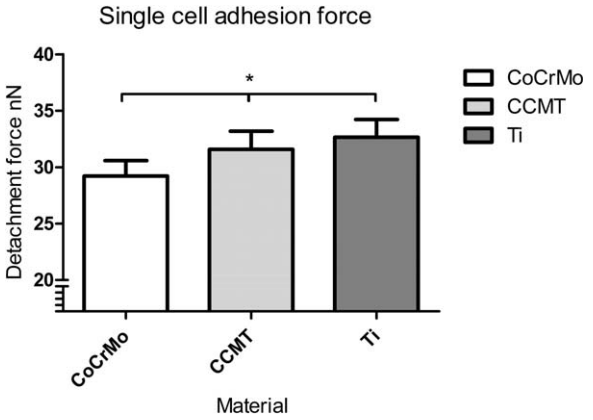

FIGURE 8. Graphical representation of the adhesion forces required to detach a single MSC from CoCrMo, CCMT, and Ti, after a 1-s dwell time on the surface of each material. The single MSC had been attached the AFM cantilever prior to the measurement via a Con-A-coated glass bead. CoCrMo had the lowest detachment force of the three materials with Ti promoting the greatest force. Each bar represents the mean ± 1SD $n = 75$, $*p < 0.0001$ material versus all other materials.

by coating the surface of the material with a thin, durable, layer of TiO_2 by atmospheric pressure CVD, thus masking the bulk alloy with the same bioactive surface oxide layer found on Ti, the current orthopedic material of choice.[5,6]

Characterization of the materials displayed an increase in wettability and surface roughness on CCMT compared to the uncoated CoCrMo. The increase in surface roughness was confirmed by SEM analysis which showed the presence of a very minor topography on CCMT in the form of shallow pits and valleys, thought to be fluctuations in the thickness of the deposited TiO_2 layer. As surface topography is known to be influential on the differentiation of MSCs[22,24,25] and has be shown to be capable of triggering bone formation without the need for additional osteogenic stimuli,[26] it is important to note this may be a contributing factor to any differences observed during *in vitro* testing, although a difference of 0.1 μm R_a is likely to have a negligible effect. There was a significant difference in roughness on the Ti control surface in comparison to both CoCrMo and CCMT, although from previous publications this surface could still be described as smooth.[22] Following TiO_2 coating, a reduction in water contact angle was observed, which may also have a positive effect on cellular response, as high surface energy substrates have previously been shown to enhance cell attachment and differentiation.[27–29] It is important to note that the variation in surface wettability on CCMT was not significant compared to that found on the positive Ti control, suggesting that while the TiO_2 layer does have an effect on the wettability of the sample, it may not fully block out the underlying material properties of the bulk CoCrMo.

Cell shape is thought to play an important role in the differentiation of MSCs.[30,31] As MSCs differentiate, it is possible to ascertain what lineage a population has committed to by studying the cytoskeletal shape of the cells and the structure of their internal f-actin stress fibres.[32] MSCs that undergo osteogenesis have been observed to change from their characteristic fibroblastic like phenotype, to a more spread spherical-star shape.[23] This phenomenon was apparent in this study, where MSCs located on the CCMT surface after 24 h, had begun f-actin reorganization, resulting in the cells appearing more spread and sprouting protrusions in the form of lamellipodia. In contrast, the majority of MSCs on CoCrMo after 24 h still appeared fibroblastic, despite the addition of osteogenic supplements to the culture media. This pattern was again evident in cell aggregates, with stress fibres appearing elongated and ordered on CoCrMo, compared to the more disordered, robust, criss-cross fibres found in aggregates on CCMT, which has been previously observed in human MSCs undergoing osteogenesis.[32] This suggests that the CCMT surface was promoting an accelerated early osteogenic response in the form of quicker cytoskeletal reorganization. By day 7, both surfaces appeared to have MSCs in the later stages of osteogenesis, indicated by the formation of thick bundles of actin located around the periphery of the cells.[23]

As MSCs differentiate along their osteogenic lineage, as well as undergoing changes in their cell shape, they excrete an ECM rich in collagen and calcium. This ECM will eventually form into bone tissue, which can be described as a vascularized mixture of inorganic calcium phosphate, also known as bone mineral or HA, and organic proteins and enzymes, such as osteopontin, osteocalcin, and bone-alkaline phosphatase.[33] Through fluorescent and colorimetric techniques, we were able to demonstrate an enhancement in various key markers of osteogenic differentiation on the CCMT surface over CoCrMo. Calcium ion and HA content were both shown to increase on CCMT compared to CoCrMo, suggesting that a greater level of bone mineralization was occurring on the TiO_2-coated substrate. A slight reduction in calcium ion content was observed from weeks 2 to 3 on CCMT when measured per cell, which can be accounted to an increase in cellular proliferation on this surface. The formation of COL-I in the ECM, which can act as a scaffold for calcium nucleation sites, was observed to be significantly reduced on CCMT in contrast to CoCrMo, to an almost comparable level as on Ti. This trend was observed in previous publications, which went on to highlight the calcium-collagen ratio in mineralized tissue, proposing that over collagenous bone tissue may be less mineralized and mechanically weak.[34]

For differentiation to occur successfully, cell attachment, and adhesion must be adequate to allow for the colonization of MSCs from surrounding tissues onto the surface of the implant. Various proteins from both the ECM and internal structure of the cell have their level of expression modified, through the cell–material interactions that occur during the adhesion process.[35] One such protein is vinculin, which plays a role in the formation of FAs by interacting with internal actin and talin.[36] FAs are best described as assemblies of proteins that congregate and co-ordinate, ordinarily around the periphery of the cell, connecting the actin of the cytoskeleton to the material while regulating signals and mechanical forces, and can be visualized by fluorescent staining of vinculin. We observed an increase in the

level of vinculin expression on CCMT and Ti, over CoCrMo at both 3 and 24 h using a pixel based quantification method. This greater level of vinculin implies that there were more FAs formed in cells on the CCMT and Ti surface, which has previously been highlighted as an important factor in osteogenic differentiation, with osteogenesis requiring large numbers of FAs compared to adipogenesis and chondrogenesis which discourage FA attachment.[18]

The visual analysis of cellular adhesion by way of confocal microscopy techniques gives a general idea of the processes that are occurring on the material surface, but cannot quantify how well adhered a single cell is to the material surface. Atomic force microscopy is an extremely powerful tool that has been used most commonly to image surfaces on the nanoscale, although recently this technique has been highlighted as a possible tool to measure the force interactions of unbinding events, for example, between cells and other biomolecules.[37] Furthermore, the resultant force curves could play a role in analyzing and identifying individual events, such as the disconnection of proteins or protein complexes during the detachment of the cell from the surface.[19] From the cell adhesion measurements performed in this study, significant differences in single cell adhesion forces between the three surfaces under physiologically relevant conditions were seen.[38] Ti and CCMT were both shown to require a significantly greater force to detach the cell from the surface following a 1-s dwell time, suggesting that these materials have superior immediate adhesion properties compared to CoCrMo, which may possibly help with the colonization of migrating cells in an *in vivo* environment.

Theoretically, the early events that take place after implantation of a device, such as interaction with the adjacent blood clot and other elements of the human body, are heavily dependent on the surface oxide layer of the material. The use of TiO_2 as a way of improving cellular response on materials has been looked at in variety of different forms. TiO_2 sol–gel dip coatings have recently been used to study the cytocompatibility of TiO_2-coated CoCrMo, where it was found that the presence of the TiO_2 layer had a reducing effect on the expression of genes involved in inflammation and oxidative stress response in human endothelial cells.[39] This effect was attributed to the TiO_2 coatings ability to reduce the release of metallic ions, specifically Co^{2+}.[40] TiO_2 nanotubes with varying dimensions have been shown to regulate MSC differentiation.[41–45] Silicon-doped TiO_2 coatings (Si-TiO_2) formed by either micro or cathodic arc oxidation, have also recently been shown to improve the response of osteogenic cells,[46,47] although it is important to point out that the Si-TiO_2 films were porous and therefore not capable of fully blocking out the underlying bulk properties of the CoCrMo. Nevertheless, the enhanced osteogenic response from Si-TiO_2 presents a possible next-step for potentially increasing the biocompatibility of CoCrMo further, via the inclusion of Si into the TiO_2 CVD coatings. Pico-to-nanometre thin TiO_2 coatings created via slow rate sputter coating of TiO_2 nanoparticles have also been shown to enhance the cellular response of osteogenic and muscle cells in the form of improved proliferation, attachment, and differentiation.[48,49] Improved proliferation and differentiation of cells isolated from the bone marrow of Sprague-Dawley rats was observed on Ti discs which had been sputter coated with TiO_2.[50] Despite the numerous positive conclusions drawn from these studies, the majority focused primarily on further increasing the biocompatibility of Ti by the addition of TiO_2. Application of TiO_2 to other biomaterials as a method of increasing their biocompatibility has yet to be fully investigated, with at present only Miyauchi et al.[51] having investigated photofunctionalized TiO_2 layers on various biomaterials and Tsaryk et al.[39] having studied the cytocompatibility of TiO_2-coated CoCrMo using human endothelial cells.

Through our preliminary work, we believe that coating less bioactive biomaterials in a layer of TiO_2 has great potential to improve the efficacy of some orthopedic implants, which need to be formed of mechanically strong, wear resistant bioinert materials, such as CoCrMo. Attempts to improve the bioactivity of CoCrMo have included forming nanophase topographies and BMP peptide immobilization, although these techniques may be difficult to upscale effectively.[11,12] Atmospheric pressure CVD not only removes the need for expensive vacuum equipment required for low pressure CVD but also is already in use industrially and therefore can be scaled up effectively. By improving the efficacy of CoCrMo, this opens up other potential applications for the use of the material.

CONCLUSION

This study analyzed the osteogenic differentiation and adhesion of human MSCs on CoCrMo, CCMT, and Ti, to ascertain whether coating CoCrMo in a layer of TiO_2 by atmospheric pressure CVD enhanced the bioactivity of the material to a comparable level as that found on Ti. The results indicated that both markers of adhesion and osteogenesis were enhanced on CCMT compared to CoCrMo, implying TiO_2 coatings may be potentially influential in the future for improving the efficacy of orthopedic implants formed of nonbioactive materials such as CoCrMo.

REFERENCES

1. Murray CJL, Richards M, Newton J, Fenton K, Anderson HR, Atkinson C, Bennett D, Bernabe E, Blencowe H, Bourne R, Braithwaite T, Brayne C, Bruce N, Brugha T, Burney P, Dherani M, Dolk H, Edmond K, Ezzati M, Flaxman A, Fleming T, Freedman G, Gunnell D, Hay,R, Hutchings S, Ohno S, Lozano R, Lyons R, Marcenes W, Naghavi M, Newton C, Pearce N, Pope D, Rushton L, Salomon J, Shibuya K, Vos T, Wang H, Williams H, Woolf A, Lopez A, Davis A. UK health performance: Findings of the Global Burden of Disease Study 2010. Lancet 2013;381:997–1020.
2. Kurtz S, Ong K, Lau E, Mowat F, Halpern M. Projections of primary and revision hip and knee arthroplasty in the United States from 2005 to 2030. J Bone Joint Surg: Am Vol 2007;89:780–785.
3. Kurtz SM, Ong KL, Schmier J, Mowat F, Saleh K, Dybvik E, Karrholm J, Garellick G, Havelin LI, Furnes O, Malchau H, Lau E. Future clinical and economic impact of revision total hip and knee arthroplasty. J Bone Joint Surg: Am Vol 2007;89A:144–151.
4. Ong KL, Mowat FS, Chan N, Lau E, Halpern MT, Kurtz SM. Economic burden of revision hip and knee arthroplasty in medicare enrollees. Clin Orthop Relat R 2006;446:22–28.
5. Geetha M, Singh AK, Asokamani R, Gogia AK. Ti based biomaterials, the ultimate choice for orthopaedic implants—A review. Prog Mater Sci 2009;54:397–425.
6. Long M, Rack HJ. Titanium alloys in total joint replacement—A materials science perspective. Biomaterials 1998;19:1621–1639.

7. Branemark PI. Osseointegration and its experimental background. J Prosthet Dent 1983;50:399–410.
8. Niinomi M. Recent metallic materials for biomedical applications. Metall Mater Trans A: Phys Metall Mater Sci 2002;33:477–486.
9. Jakobsen SS, Baas J, Jakobsen T, Soballe K. Acid etching does not improve CoCrMo implant osseointegration in a canine implant model. Hip Int 2010;20:171–178.
10. Hinuber C, Kleemann C, Friederichs RJ, Haubold L, Scheibe HJ, Schuelke T, Boehlert C, Baumann MJ. Biocompatibility and mechanical properties of diamond-like coatings on cobalt–chromium–molybdenum steel and titanium–aluminum–vanadium biomedical alloys. J Biomed Mater Res A 2010;95A:388–400.
11. Poh CK, Shi ZL, Tan XW, Liang ZC, Foo XM, Tan HC, Neoh KG, Wang W. Cobalt chromium alloy with immobilized BMP peptide for enhanced bone growth. J Orthop Res 2011;29:1424–1430.
12. Webster TJ, Ejiofor JU. Increased osteoblast adhesion on nanophase metals: Ti, Ti6Al4V, and CoCrMo. Biomaterials 2004;25: 4731–4739.
13. Textor M, Sittig C, Frauchiger V, Tosatti S, Brunette DM. Properties and biological significance of natural oxide films on titanium and its alloys. In: Brunette DM, Tengvall P, Textor M, Thomsen P, editors. Titanium in Medicine. New York: Springer; 2001. p 172–230.
14. Diebold U. The surface science of titanium dioxide. Surf Sci Rep 2003;48:53–229.
15. Pittenger MF, Douglas R, Mackay AM, Beck SC, Jaiswal RK, Mosca JD, Moorman MA, Simonetti DW, Craig S, Marshak DR. Multilineage potential of adult human mesenchymal stem cells. Science 1999;284:143–147.
16. Davies JE. Mechanisms of endosseous integration. Int J Prosthodont 1998;11:391–401.
17. Davies JE. Understanding peri-implant endosseous healing. J Dent Educ 2003;67:932–949.
18. Mathieu PS, Loboa EG. Cytoskeletal and focal adhesion influences on mesenchymal stem cell shape, mechanical properties, and differentiation down osteogenic, adipogenic, and chondrogenic pathways. Tissue Eng Part B: Rev 2012;18:436–444.
19. Weder G, Voros J, Giazzon M, Matthey N, Heinzelmann H, Liley M. Measuring cell adhesion forces during the cell cycle by force spectroscopy. Biointerphases 2009;4:27–34.
20. Cross AJ, Dunnill CW, Parkin IP. Production of predominantly anatase thin films on various grades of steel and other metallic substrates from $TiCl_4$ and ethyl acetate by atmospheric pressure CVD. Chem Vapor Depos 2012;18:133–139.
21. Hyett G, Darr JA, Mills A, Parkin IP. An investigation into the optimum thickness of titanium dioxide thin films synthesized by using atmospheric pressure chemical vapour deposition for use in photocatalytic water oxidation. Chem Eur J 2010;16:10546–10552.
22. Wennerberg A, Albrektsson T. Effects of titanium surface topography on bone integration: A systematic review. Clin Oral Implan Res 2009;20:172–184.
23. Rodriguez JP, Gonzalez M, Rios S, Cambiazo V. Cytoskeletal organization of human mesenchymal stem cells (MSC) changes during their osteogenic differentiation. J Cell Biochem 2004;93:721–731.
24. Shalabi MM, Gortemaker A, Van't Hof MA, Jansen JA, Creugers NHJ. Implant surface roughness and bone healing: A systematic review. J Dent Res 2006;85:496–500.
25. Logan N, Brett P. The Control of Mesenchymal Stromal Cell Osteogenic Differentiation through Modified Surfaces. Stem Cells Int 2013;2013:361637.
26. Dalby MJ, Gadegaard N, Tare R, Andar A, Riehle MO, Herzyk P, Wilkinson CDW, Oreffo ROC.. The control of human mesenchymal cell differentiation using nanoscale symmetry and disorder. Nat Mater 2007;6:997–1003.
27. Zhao G, Schwartz Z, Wieland M, Rupp F, Geis-Gerstorfer J, Cochran DL, Boyan BD. High surface energy enhances cell response to titanium substrate microstructure. J Biomed Mater Res A 2005;74A:49–58.
28. Lai HC, Zhuang LF, Liu X, Wieland M, Zhang ZY. The influence of surface energy on early adherent events of osteoblast on titanium substrates. J Biomed Mater Res A. 2010;93A:289–296.
29. Sawase T, Jimbo R, Baba K, Shibata Y, Ikeda T, Atsuta M. Photo-induced hydrophilicity enhances initial cell behavior and early bone apposition. Clin Oral Implan Res 2008;19:491–496.
30. Kilian KA, Bugarija B, Lahn BT, Mrksich M. Geometric cues for directing the differentiation of mesenchymal stem cells. Proc Natl Acad Sci USA 2010;107:4872–4877.
31. McBeath R, Pirone DM, Nelson CM, Bhadriraju K, Chen CS. Cell shape, cytoskeletal tension, and RhoA regulate stem cell lineage commitment. Dev Cell 2004;6:483–495.
32. Yourek G, Hussain MA, Mao JJ. Cytoskeletal changes of mesenchymal stem cells during differentiation. Asaio J 2007;53:219–228.
33. Golub EE, Boesze-Battaglia K. The role of alkaline phosphatase in mineralization. Curr Opin Orthop 2007;18:444–448.
34. Khan MR, Donos N, Salih V, Brett PM. The enhanced modulation of key bone matrix components by modified Titanium implant surfaces. Bone 2012;50:1–8.
35. Anselme K. Osteoblast adhesion on biomaterials. Biomaterials. 2000;21:667–681.
36. Humphries JD, Wang P, Streuli C, Geiger B, Humphries MJ, Ballestrem C. Vinculin controls focal adhesion formation by direct interactions with talin and actin. J Cell Biol 2007;179:1043–1057.
37. Francis LW, Lewis PD, Wright CJ, Conlan RS. Atomic force microscopy comes of age. Biol Cell 2010;102:133–143.
38. Friedrichs J, Helenius J, Muller DJ. Quantifying cellular adhesion to extracellular matrix components by single-cell force spectroscopy. Nat Protoc 2010;5:1353–1361.
39. Tsaryk R, Peters K, Unger RE, Feldmann M, Hoffmann B, Heidenau F, Kirkpatrick CJ. Improving cytocompatibility of Co28Cr6Mo by TiO_2 coating: Gene expression study in human endothelial cells. J R Soc Interface 2013;10:20130428.
40. Hoffmann B, Feldmann M, Ziegler G. Sol–gel and precursor-derived coatings with cover function on medical alloys. J Mater Chem 2007;17:4034–4040.
41. Brammer KS, Frandsen CJ, Jin S. TiO_2 nanotubes for bone regeneration. Trends Biotechnol 2012;30:315–322.
42. Park J, Bauer S, von der Mark K, Schmuki P. Nanosize and vitality: TiO_2 nanotube diameter directs cell fate. Nano Lett 2007;7: 1686–1691.
43. Park J, Bauer S, Schlegel KA, Neukam FW, von der Mark K, Schmuki P. TiO_2 nanotube surfaces: 15 nm—An optimal length scale of surface topography for cell adhesion and differentiation. Small 2009;5:666–671.
44. Lai M, Cai KY, Zhao L, Chen XY, Hou YH, Yang ZX. Surface functionalization of TiO_2 nanotubes with bone morphogenetic protein 2 and its synergistic effect on the differentiation of mesenchymal stem cells. Biomacromolecules 2011;12:1097–1105.
45. Oh S, Brammer KS, Li YSJ, Teng D, Engler AJ, Chien S, Jin S. Stem cell fate dictated solely by altered nanotube dimension. Proc Natl Acad Sci USA 2009;106:2130–2135.
46. Wang B, Sun J, Qian S, Liu X, Zhang S, Liu F, Dong S, Zha G. Proliferation and differentiation of osteoblastic cells on silicon-doped TiO(2) film deposited by cathodic arc. Biomed Pharmacother 2012;66:633–641.
47. Wang Q, Hu H, Qiao Y, Zhang Z, Sun J. Enhanced performance of osteoblasts by silicon incorporated porous TiO_2 coating. J Mater Sci Technol 2012;28:109–117.
48. Sugita Y, Ishizaki K, Iwasa F, Ueno T, Minamikawa H, Yamada M, Suzuki T, Ogawa T. Effects of pico-to-nanometer-thin TiO_2 coating on the biological properties of microroughened titanium. Biomaterials 2011;32:8374–8384.
49. Ishizaki K, Sugita Y, Iwasa F, Minamikawa H, Ueno T, Yamada M, Suzuki T, Ogawa T. Nanometer-thin TiO_2 enhances skeletal muscle cell phenotype and behavior. Int J Nanomed 2011;6:2191–2203.
50. Tsukimura N, Kojima N, Kubo K, Att W, Takeuchi K, Kameyama Y, Maeda H, Ogawa T. The effect of superficial chemistry of titanium on osteoblastic function. J Biomed Mater Res A 2008;84: 108–116.
51. Miyauchi T, Yamada M, Yamamoto A, Iwasa F, Suzawa T, Kamijo R, Baba K, Ogawa T. The enhanced characteristics of osteoblast adhesion to photofunctionalized nanoscale TiO_2 layers on biomaterials surfaces. Biomaterials 2010;31:3827–3839.